Xing Fu,[1] Meijun Zhu,[2] Shuming Zhang,[2] Marc Foretz,[3,4,5] Benoit Viollet,[3,4,5] and Min Du[1]

Obesity Impairs Skeletal Muscle Regeneration Through Inhibition of AMPK

Diabetes 2016;65:188–200 | DOI: 10.2337/db15-0647

Obesity is increasing rapidly worldwide and is accompanied by many complications, including impaired muscle regeneration. The obese condition is known to inhibit AMPK activity in multiple tissues. We hypothesized that the loss of AMPK activity is a major reason for hampered muscle regeneration in obese subjects. We found that obesity inhibits AMPK activity in regenerating muscle, which was associated with impeded satellite cell activation and impaired muscle regeneration. To test the mediatory role of AMPKα1, we knocked out AMPKα1 and found that both proliferation and differentiation of satellite cells are reduced after injury and that muscle regeneration is severely impeded, reminiscent of hampered muscle regeneration seen in obese subjects. Transplanted satellite cells with AMPKα1 deficiency had severely impaired myogenic capacity in regenerating muscle fibers. We also found that attenuated muscle regeneration in obese mice is rescued by AICAR, a drug that specifically activates AMPK, but AICAR treatment failed to improve muscle regeneration in obese mice with satellite cell–specific AMPKα1 knockout, demonstrating the importance of AMPKα1 in satellite cell activation and muscle regeneration. In summary, AMPKα1 is a key mediator linking obesity and impaired muscle regeneration, providing a convenient drug target to facilitate muscle regeneration in obese populations.

Skeletal muscle, which accounts for 40% of body mass, is responsible for locomotion and is the major site for glucose and fatty acid utilization, playing a key role in preventing obesity and type 2 diabetes (1–3). Skeletal muscle regeneration is an integrated part of the physiological process in skeletal muscle. In both exercise-induced muscle damage and muscle trauma, skeletal muscle regeneration is required for recovery after injury (4,5). Moreover, sustained but attenuated muscle regeneration is indispensable in the etiology of muscular diseases, such as Duchenne muscular dystrophy (6).

Satellite cells are the major postnatal myogenic cells in skeletal muscle (7). In response to muscle damage, satellite cells are activated and undergo asymmetric division, with one daughter cell to replenish the original cell and the other cell to undergo myogenic differentiation (8). The myogenic cells then fuse with damaged muscle fibers to repair or form new muscle fibers to replace the necrotic ones. Improper muscle regeneration leads to muscle atrophy and impairment of muscle contractile function (9–11). On the other hand, successful muscle regeneration requires both sufficient quantity and proper myogenic differentiation of satellite cells (12). Proliferation of satellite cells is regulated by growth factors (13), whereas myogenic differentiation is regulated by myogenic regulatory factors (MRFs), including Myf5, MyoD, myogenin, and MRF4 (3); disrupted expression of MRFs negatively affects muscle regeneration (14).

AMPK is known for its regulatory role in energy metabolism (15). Metabolic disorders such as obesity and type 2 diabetes have become major health problems worldwide and are associated with attenuated muscle regeneration (16,17) and reduced AMPK activity (18). However, the role of AMPK in impaired muscle regeneration due to obesity and type 2 diabetes has not been defined. AMPK is a heterotrimeric enzyme with an α-catalytic

[1]Washington Center for Muscle Biology, Department of Animal Sciences and Department of Pharmaceutical Sciences, Washington State University, Pullman, WA
[2]School of Food Science, Washington State University, Pullman, WA
[3]INSERM U1016, Institut Cochin, Paris, France
[4]Université Paris Descartes, Sorbonne Paris Cité, Paris, France
[5]CNRS UMR 8104, Paris, France
Corresponding author: Min Du, min.du@wsu.edu.

Received 15 May 2015 and accepted 10 September 2015.
This article contains Supplementary Data online at http://diabetes.diabetesjournals.org/lookup/suppl/doi:10.2337/db15-0647/-/DC1.

subunit and two isoforms, α1 and α2 (19). We previously identified the stimulatory effect of AMPKα1, the dominant AMPKα isoform in satellite cells, on myogenin expression and fusion into myotubes (20,21), which led us to hypothesize that AMPKα1 facilitates muscle regeneration and that obesity impedes muscle regeneration mainly through inhibition of AMPK. In the present study, we found that the lack of AMPKα1 activity reduces the density of satellite cells and their differentiation after muscle injury and that activation of AMPK rescues muscle regeneration in obese mice. Thus, AMPK is a therapeutic target for facilitating muscle regeneration in patients with obesity and diabetes, whereas AMPK is inhibited.

RESEARCH DESIGN AND METHODS

Induction of AMPKα1 Knockout in $R26^{Cre}/AMPK\alpha1^{fl/fl}$ Mice and $Pax7^{Cre}/AMPK\alpha1^{fl/fl}$ Mice

Three- to 4-month-old $R26^{Cre}/AMPK\alpha1^{fl/fl}$ mice and $Pax7^{Cre}/AMPK\alpha1^{fl/fl}$ mice were injected intraperitoneally with tamoxifen 100 mg per 1 kg body weight per day for 5 continuous days to induce AMPKα1 knockout (KO) (22). $AMPK\alpha1^{fl/fl}$ mice treated with tamoxifen were used as controls. Mice were allowed to rest for at least 3 days after the last tamoxifen injection before further experiments.

Induction of Muscle Regeneration

To induce muscle regeneration, 100 μL of 10 μmol/L cardiotoxin (CTX) was injected into each tibialis anterior (TA) muscle of 3–4-month-old mice (10,21).

FACS

TA muscle was digested in DMEM with collagenase D and dispase II as previously described (21). Cells were blocked in anti-mouse CD16/CD32 antibody and then stained with anti-mouse CD45 PE-Cy7, anti-mouse TER119 PE-Cy7, anti-mouse CD31 PE-Cy7, anti-mouse Sca-1 APC-Cy7, and anti-mouse integrin α7 APC antibodies or anti-mouse F4/80 Alexa Fluor 488 and anti-mouse Ly6G/C APC antibodies. Stained cells were sorted on FACSaria (BD Biosciences, San Jose, CA) and analyzed by FlowJo (Tree Star, Inc., San Carlos, CA). Gates were made based on Fluorescence Minus One control (Supplementary Fig. 2).

Oil Red O Staining

Oil red O staining was performed as previously described (10). Briefly, cells were fixed in 10% formalin for 30 min, stained with oil red O in 60% isopropanol for 10 min, and counterstained with hematoxylin. Adipogenic efficiency was calculated by dividing the number of oil red O–positive cells by the number of total cells.

Real-Time Quantitative PCR

cDNA was synthesized using a reverse transcription kit (Bio-Rad, Hercules, CA). Primers are listed in Supplementary Table 1. Real-time PCR (RT-PCR) was carried out using a CFX RT-PCR detection system (Bio-Rad) with a SYBR Green RT-PCR kit (Bio-Rad). After amplification, a melting curve (0.01°C/s) was used to confirm product purity, and agarose gel electrophoresis was performed to confirm that only a single product of the correct size was amplified. Relative mRNA content was normalized to 18S rRNA content (21).

Immunoblotting Analysis

Immunoblotting analysis was performed as previously described using an Odyssey Infrared Imaging System (Model 9120, LI-COR Biosciences, Lincoln, NE) (23). Band density was normalized to β-tubulin content.

Immunocytochemical Staining

Cells grown on multiple-well plates were fixed in cold methanol for 10 min, permeabilized with 0.1% Triton X-100 for 5 min, blocked with 1% BSA, and incubated with primary antibodies at 4°C overnight. Cells were then stained with corresponding secondary antibodies (1:1,000) for 1 h. Images were taken using an EVOS microscope.

Immunohistochemical Staining

TA muscle fixed in 4% paraformaldehyde or fresh TA muscle was frozen in isopentane cooled in liquid nitrogen. Frozen tissue was sectioned (10 μm thick). Sections of fixed tissue were heated in citrate buffer for 20 min, blocked with 5% goat serum in TBS containing 0.3% Triton X-100 for 2 h, and stained with primary antibodies overnight and corresponding fluorescent secondary antibodies for 1 h. Sections of unfixed tissue were stained without antigen retrieval. Sections were then mounted in a mounting medium (Vector Laboratories, Burlingame, CA).

Quantification of $Pax7^+$ Satellite Cells and Embryonic Myosin Heavy Chain–Positive Muscle Fibers

$Pax7^+$ cells with nuclei identified by DAPI staining were classified as satellite cells. For each TA muscle sample, the total number of satellite cells and embryonic myosin heavy chain–positive (EMH^+) muscle fibers on four randomly selected microscopic fields of each of three sections at various depths of muscle were counted (four fields per section, three sections per muscle). Average numbers obtained from the three examined sections of each muscle sample were used as a biological replicate for comparative analysis.

Statistics

All data are expressed as mean ± SEM. Data were analyzed using the general linear model in SAS statistical software (Version 9.2, SAS Institute Inc., Cary, NC), and the *t* or Tukey range test was used to determine significance of differences among means. $P < 0.05$ was considered significant.

RESULTS

Diet-Induced Obesity Is Associated With Reduced AMPK Activity in Satellite Cells During Muscle Regeneration

We previously reported that AMPKα1 is the dominant α-subunit in myogenic cells and that lack of AMPKα1 attenuates myogenic differentiation (Supplementary Fig. 1*A*) (20,21). AMPK activity has also been reported to be inhibited in multiple tissues of obese rodents and humans

(24,25). To test whether AMPK activity was downregulated in muscle of obese mice, which attenuated muscle regeneration, C57BL/6 mice were fed a 60% high-fat diet for 3 months to induce obesity (Fig. 1*A–C*). Damage to TA muscle was induced by CTX injection. The p-AMPKα/AMPKα and p-ACC/ACC ratios were lower in regenerating muscle from obese mice than that from control mice at 3 days postinjury, indicating a lower AMPK activity in muscle of obese mice after injury (Supplementary Fig. 2*A*). However, no difference was found in uninjured muscle between control and obese mice (Supplementary Fig. 2*B*). Due to different cell composition in uninjured and injured muscle, satellite cells were isolated from injured muscle of control and obese mice to better understand the change of AMPK activity in these cells. No difference was detected, which could be the result of the isolation process and the following in vitro culture that diminished the difference (Supplementary Fig. 2*C*). Immunohistochemical (IHC) staining, therefore, was performed to examine the p-AMPKα level in satellite cells in vivo. AMPKα1 expression was detected in satellite cells in both uninjured and injured muscle (Fig. 1*D*). However, p-AMPKα was only detected in satellite cells in injured muscle, suggesting an activation of AMPK in satellite cells after injury (Fig. 1*D*). Of note, more satellite cells stained positive for p-AMPKα in injured muscle from control mice than from obese mice, indicating that AMPK activation in satellite cells after injury is negatively affected in obese mice (Fig. 1*D* and *E*).

No difference in the expression of AMPKα1 and -α2 subunits was found between satellite cells isolated from control and obese mice during muscle regeneration (Supplementary Fig. 2*D* and *E*) or in the expression of the two AMPK kinases LKB1 and CAMKK2 (Supplementary Fig. 2*F*). In addition, the ATP/AMP ratio was not different between injured muscle from control and that from obese mice, showing that AMPK activation pathways were not affected in satellite cells as a result of obesity (Supplementary Fig. 2*G*). Moreover, no difference in muscle fiber composition was found between control and obese mice, which rules out the possible influence of altered muscle fiber composition in muscle regeneration (Supplementary Fig. 2*H*).

Tumor necrosis factor-α (TNFα) downregulates AMPK activity in muscle (18), and muscle regeneration involves infiltration of macrophages that secrete cytokines, including TNFα (26,27). An increase of macrophage infiltration was observed in obese mice as measured by FACS, but no difference was found in the ratio of M1 to M2 macrophages, suggesting no defect in macrophage polarization (Fig. 1*F* and Supplementary Fig. 3*A* and *B*) (28). Consistently, the expression of TNFα, an M1 macrophage marker, and transforming growth factor-β (TGFβ), an M2 macrophage marker, were both higher in injured muscle from obese compared with control mice (Fig. 1*G*). To test whether TNFα affects AMPK activity in satellite cells, isolated satellite cells were treated with TNFα 10 ng/mL, which reduced p-AMPKα levels in satellite cells; in contrast, 125 μmol/L AICAR neutralized the negative effect of TNFα on AMPKα phosphorylation (Fig. 1*H*).

Diet-Induced Obesity Attenuates Muscle Regeneration

Muscle regeneration in control and obese mice was then compared. At 3 days postinjury, most muscle fibers were necrotic in muscle from both control and obese mice, which were enlarged and lightly stained by hematoxylin-eosin (H-E) (Fig. 2*B*). However, regenerating muscle of control mice contained many more newly formed fibers, which was confirmed by IHC staining against EMH, a marker of regenerated fibers (3) (Fig. 2*A* and *B*). The difference was also observed at 7 days postinjury. Although well-restored muscle structure with new fibers was observed in control mice, a much smaller number of regenerated fibers and poorly restored structure were seen in obese mice (Fig. 2*C* and *E*). Consistently, at 3 days postinjury, the expression of genes important for myogenesis, including Pax7 and MRFs (Myf5, MyoD, and myogenin), was lower in regenerating muscle from obese than from control mice (Fig. 2*E*). However, myogenic differentiation was not different between isolated satellite cells of control and obese mice possibly because of the lack of difference in AMPK activity in vitro (Supplementary Fig. 2*I*). Satellite cells are indispensable for muscle regeneration (29). The density of $Pax7^+$ satellite cells was lower in muscle from obese than from control mice at both 3 and 7 days postinjury, indicating a reduced satellite cell population (Fig. 2*F* and *G*). In agreement, FACS showed that $CD45^-/TER119^-/CD31^-$ (Lin^-)$Sca\text{-}1^-$/integrin $\alpha7^+$ satellite cells were less in muscle of obese mice than in control mice, indicating that the reduced satellite cell pool might contribute to attenuated muscle regeneration (Fig. 2*H* and Supplementary Fig. 3*C*) (30).

To further trace muscle regeneration, we used *Pax7^{Cre}/tdomato,EGFP* mice in which satellite cells and their derived myogenic cells and regenerated muscle fibers carry green fluorescence after tamoxifen treatment. Obesity reduced the number of green fluorescent fibers in regenerating muscle at 3 and 7 days postinjury compared with the control condition (Supplementary Fig. 4*A* and *B*).

Muscle Regeneration in AMPKα1 KO Mice Was Attenuated

Because of the dominant expression of AMPKα1 in satellite cells and the reduced AMPK activity in activated satellite cells from obese mice, we hypothesized that attenuated muscle regeneration in obese mice is due to reduced AMPKα1 activity in satellite cells (Supplementary Figs. 1*A* and 2*D*). A mouse strain with constitutional AMPKα1 KO was used to mimic the inhibition in AMPK activity during muscle regeneration due to obesity. At 3 days postinjury, fewer newly formed muscle fibers were found in AMPKα1 KO than in wild-type (WT) mice as shown by H-E and IHC staining (Supplementary Fig. 5*A* and *B*). At 7 days postinjury, better restoration of muscle structure with fewer necrotic muscle fibers and more

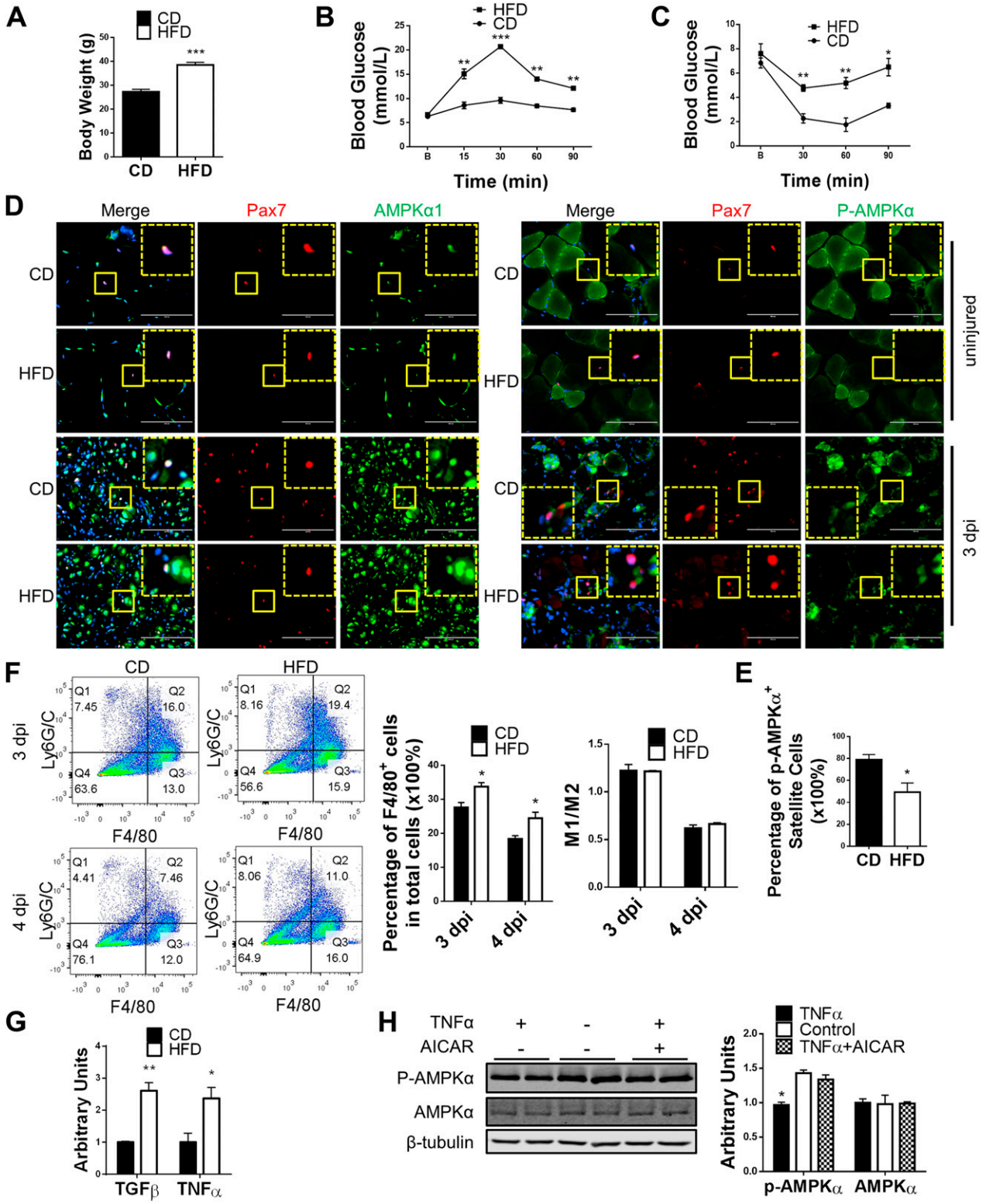

Figure 1—Reduced AMPK activity in satellite cells of obese mice during muscle regeneration. *A*: Body weight of male mice fed a control diet (CD) and a high-fat diet (HFD). *B*: Glucose tolerance test of CD and HFD mice. *C*: Insulin tolerance test of CD and HFD mice. *D*: IHC staining identifying AMPKα1 expression and p-AMPKα level in satellite cells of muscle before injury and 3 days postinjury (dpi). The dotted-line inset on each image shows magnification of the area marked by the solid-line box. Scale bars = 100 μm. *E*: Quantification of satellite cells staining positive for p-AMPKα in muscle of CD and HFD mice 3 dpi. *F*: FACS identifying M1 (Q2) and M2 (Q3) macrophages in regenerating muscle of CD and HFD mice. *G*: RT-PCR of TGFβ and TNFα expression in muscle of CD and HFD mice at 3 dpi. *H*: Western blot analysis of p-AMPKα and AMPKα levels in WT satellite cells treated with 10 ng/mL TNFα with and without 125 μmol/L AICAR for 12 h and untreated control. Data are mean ± SEM (n = 3). *P < 0.05, **P < 0.01, ***P < 0.0001 vs. control.

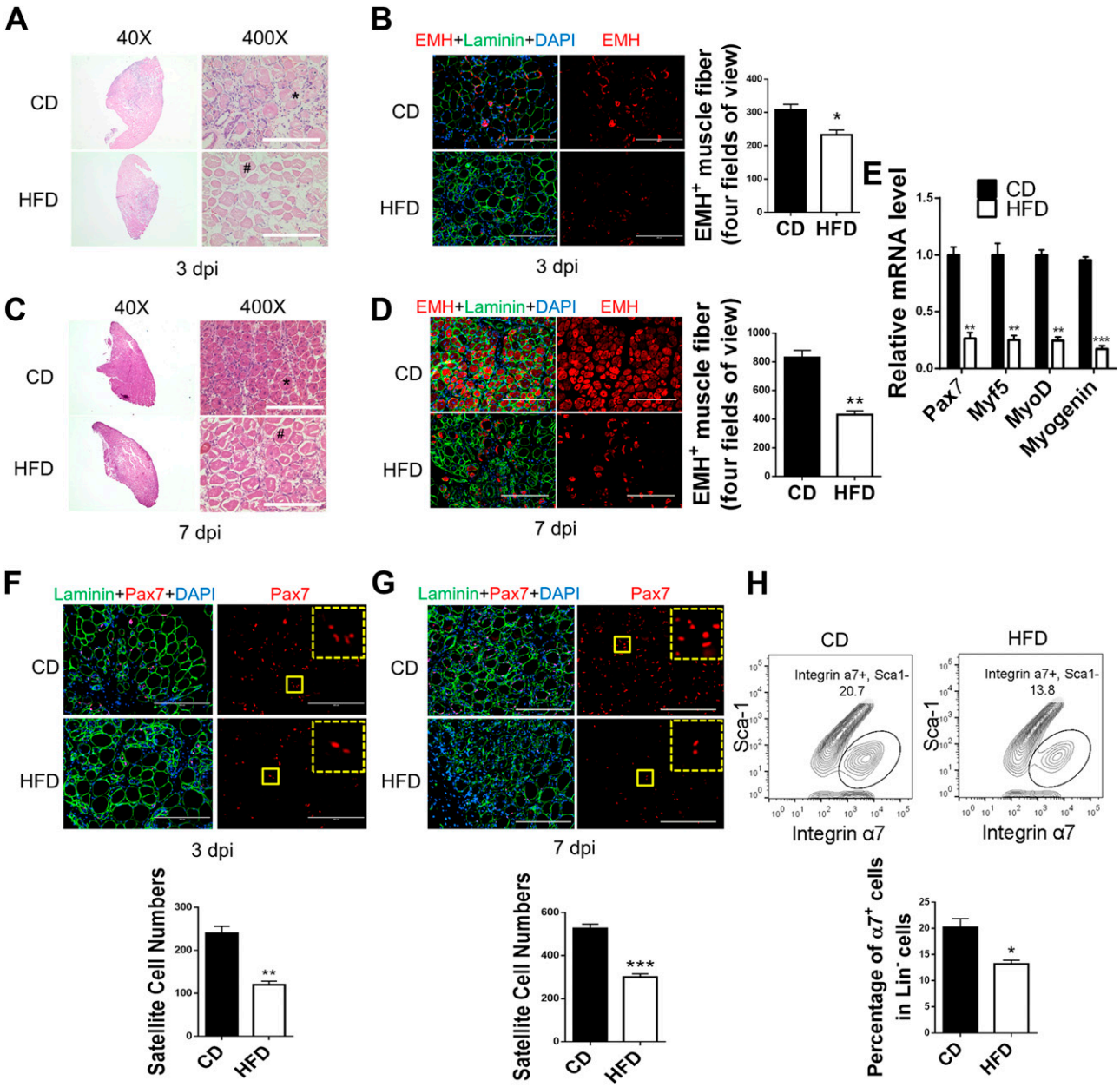

Figure 2—Attenuated muscle regeneration in mice with diet-induced obesity. TA muscle of mice fed a control diet (CD) and a high-fat diet (HFD) were injured by CTX injection. *A*: Regeneration of TA muscle at 3 days postinjury (dpi) examined by H-E staining showing necrotic muscle fibers (#) and regenerating muscle fibers (*). *B*: IHC staining of EMH^+ muscle fibers in TA muscle at 3 dpi and quantification. *C*: Regeneration of TA muscle at 7 dpi examined by H-E staining showing necrotic muscle fibers (#) and regenerating muscle fibers (*). *D*: IHC staining of EMH^+ muscle fibers in TA muscle at 7 dpi and quantification. *E*: Pax7, Myf5, MyoD, and myogenin mRNA levels in TA muscle at 3 dpi. *F* and *G*: IHC staining of $Pax7^+$ satellite cells in TA muscle at 3 dpi (*F*) and 7 dpi (*G*) and quantification. The dotted-line inset on each image shows magnification of the area marked by the solid-line box. *H*: FACS for $Lin^-/Sca\text{-}1^-/integrin\ \alpha7^+$ satellite cells in TA muscle at 7 dpi. Data are mean ± SEM (n = 3). Scale bars = 200 μm. $^*P < 0.05$, $^{**}P < 0.01$, $^{***}P < 0.0001$ vs. control.

regular-shaped muscle fibers was observed in WT than in AMPKα1 KO mice (Fig. 3*A* and *B*). Consistently, at 14 days postinjury, while many necrotic muscle fibers and immature muscle fibers remained in the muscle of AMPKα1 KO mice, muscle structure was restored in WT mice with only a few EMH^+ muscle fibers close to normal size remaining, indicating better regeneration than in AMPKα1 KO mice (Fig. 3*A* and *B*).

Satellite Cell Density in Undamaged Muscle and Regenerating Muscle of AMPKα1 KO Mice Was Lower Than in WT Mice

We then tested whether AMPKα1 ablation alters satellite cell population in muscle during muscle regeneration. As expected, IHC staining showed that the density of $Pax7^+$ satellite cells was lower in AMPKα1 KO than in WT mice at 3, 7, and 14 days postinjury (Fig. 3*C* and Supplementary

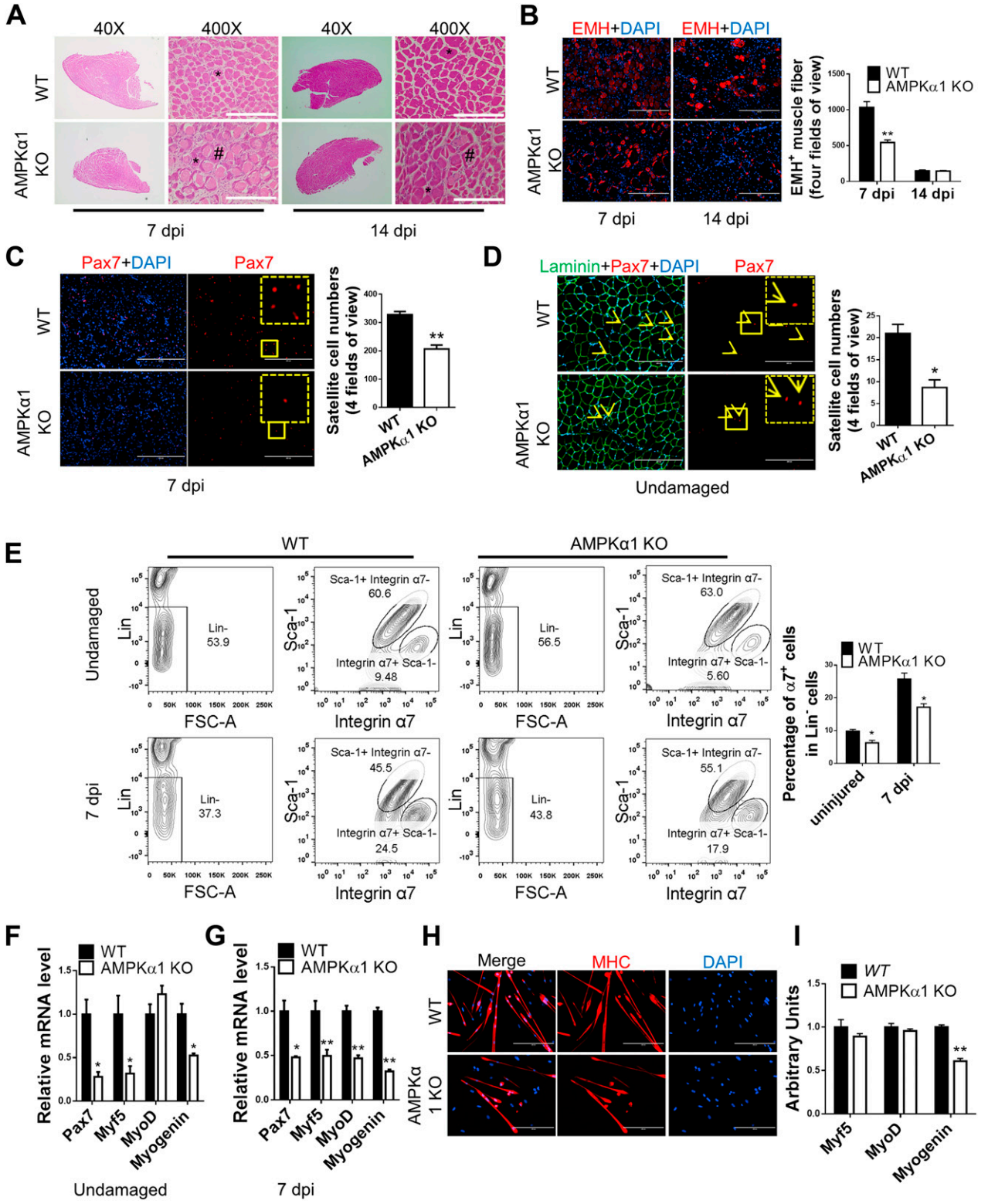

Figure 3—Impaired muscle regeneration efficiency in AMPKα1 KO mice. TA muscle of WT and AMPKα1 KO mice was injured by CTX injection. *A*: Regeneration of TA muscle at 7 and 14 days postinjury (dpi) examined by H-E staining showing necrotic muscle fibers (#) and regenerating muscle fibers (*). *B*: EMH$^+$ muscle fibers in TA muscle at 7 and 14 dpi detected by IHC staining and quantification of EMH$^+$ muscle fibers. *C* and *D*: IHC staining for Pax7$^+$ satellite cells (arrowheads) in TA muscle at 7 dpi (*C*) and before injury (*D*). The dotted-line inset on each image shows magnification of the area marked by the solid-line box. *E*: FACS for Lin$^-$/Sca-1$^-$/integrin α7$^+$ satellite cells in TA muscle before injury and at 7 dpi. *F* and *G*: Pax7, Myf5, MyoD, and myogenin mRNA levels before injury (*F*), and 7 dpi (*G*). *H*: Myogenic differentiation of Lin$^-$/Sca-1$^-$/integrin α7$^+$ cells isolated from undamaged muscle measured by immunocytochemical staining for myosin heavy chain (MHC). *I:* Myf5, MyoD, and myogenin mRNA levels in WT satellite cells and AMPKα1 KO satellite cells 1 day after induction of myogenic differentiation. Data are mean ± SEM (n = 3). Scale bars = 200 μm. *P < 0.05, **P < 0.01 vs. control.

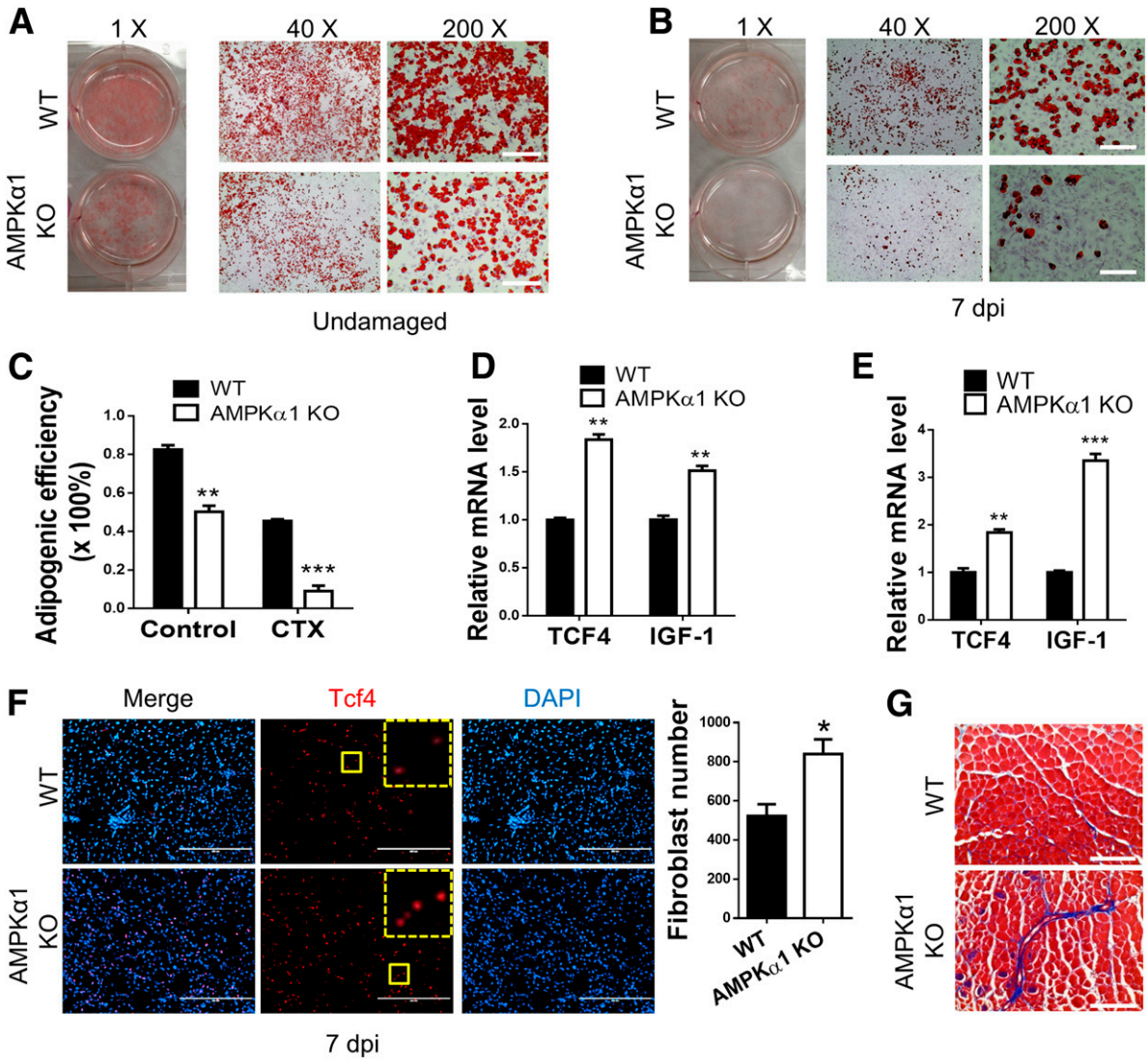

Figure 4—Enhanced fibrogenesis by AMPKα1 KO in muscle during regeneration. *A* and *B*: Adipogenic differentiation of Lin$^-$/Sca-1$^+$ cells isolated from undamaged WT and AMPKα1 KO muscle (*A*) and from WT and AMPKα1 KO muscle at 7 days postinjury (dpi) (*B*) as measured by oil red O staining. *C*: Quantified adipogenic efficiencies of Lin$^-$/Sca-1$^+$ cells shown in *A* and *B* expressed as percentage of oil red O–positive cells. *D*: TCF4 and IGF-I mRNA levels in WT and AMPKα1 KO nonmyogenic cells isolated from muscle at 7 dpi. *E*: TCF4 and IGF-I mRNA levels in WT and AMPKα1 KO muscle at 7 dpi. *F*: IHC staining of Tcf4$^+$ fibroblasts in WT and AMPKα1 KO regenerating muscle at 7 dpi. The dotted-line inset on each image shows magnification of the area marked by the solid-line box. *G*: Trichrome staining of WT and AMPKα1 KO TA sections at 14 dpi. Data are mean ± SEM (n = 3). Scale bars = 200 μm. *P < 0.05, **P < 0.01, ***P < 0.0001 vs. control.

Fig. 5*C* and *D*). In agreement, Lin$^-$/Sca-1$^-$/integrin α7$^+$ satellite cells were reduced in AMPKα1 KO muscle (Fig. 3*E*). Consistently, the density of satellite cells was also lower in undamaged muscle of AMPKα1 KO than in WT mice (Fig. 3*D* and *E*). These data suggest that the reduced satellite cell population in AMPKα1 KO mice during muscle regeneration was partially the result of the reduced satellite population in AMPKα1 KO mice before muscle injury.

Expression of Myogenic Genes Was Reduced in AMPKα1 KO Regenerating Muscle

Because of the reduced satellite cell population and hampered muscle structure restoration, we wondered whether the transcription of Pax7 and MRFs was also affected due to AMPKα1 KO. In undamaged muscle, transcription levels of Pax7, Myf5, and myogenin were lower in AMPKα1 KO than in WT muscle (Fig. 3*F*), which could be attributed to reduced satellite cell number due to AMPKα1 KO (20,21). At 3 and 7 days postinjury, all tested MRFs were transcribed at lower levels in AMPKα1 KO than in WT muscle, except the MyoD level at 3 days postinjury (P = 0.077) (Fig. 3*G* and Supplementary Fig. 5*E*). Lin$^-$/Sca-1$^-$/integrin α7$^+$ satellite cells were isolated from TA muscle of WT and AMPKα1 KO mice, and their myogenic differentiation was found to be impaired due to AMPKα1 KO (Fig. 3*H* and *I*). In aggregate, these data show that impaired

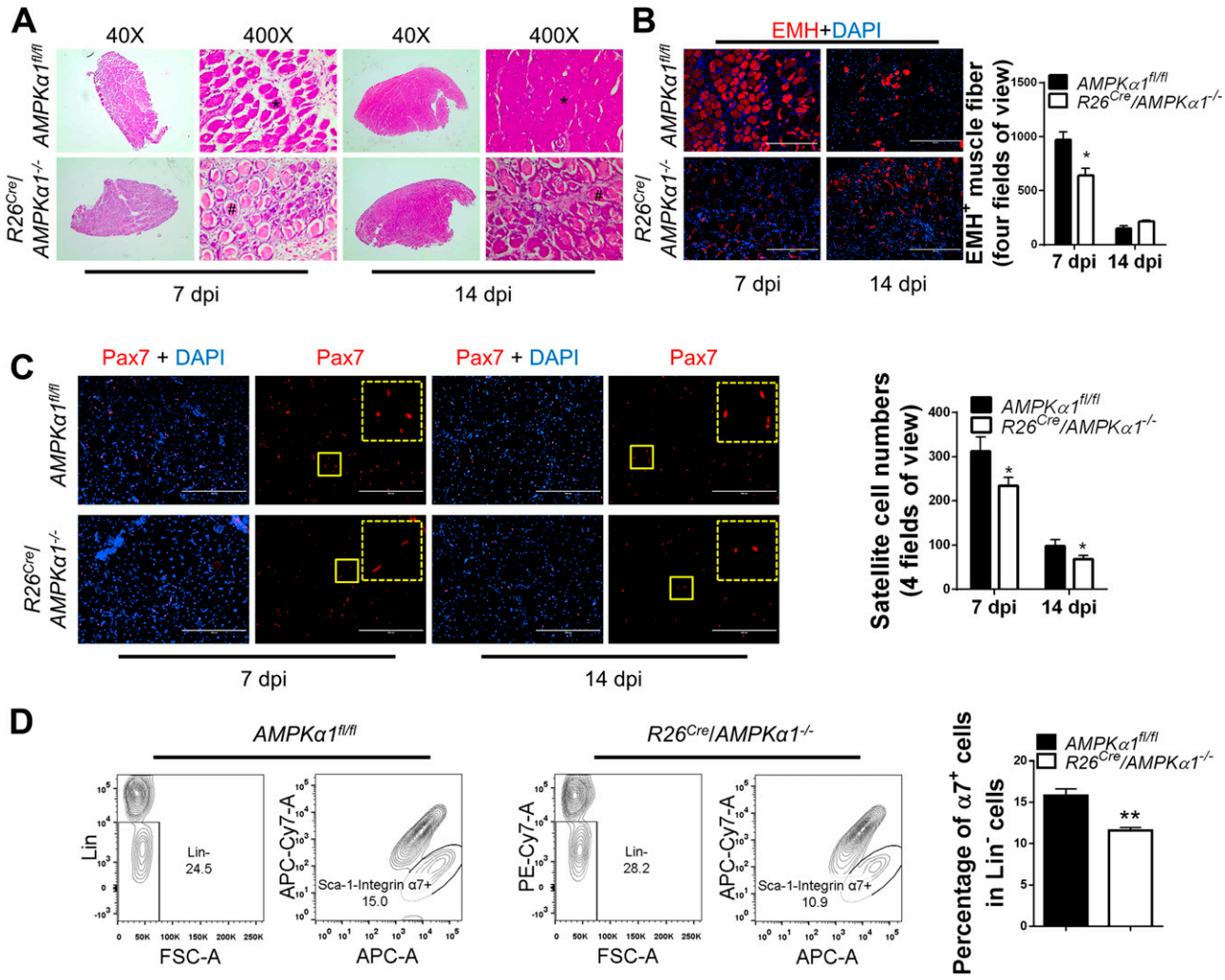

Figure 5—Impaired muscle regeneration efficiency in conditional AMPKα1 KO mice. TA muscle of tamoxifen-treated *AMPKα1$^{fl/fl}$* mice and conditional AMPKα1 KO (*R26^{Cre}/AMPKα1$^{-/-}$*) mice were injured by CTX injection. *A*: Regeneration of TA muscle at 7 and 14 days postinjury (dpi) examined by H-E staining showing necrotic muscle fibers (#) and regenerating muscle fibers (*). *B*: EMH$^+$ muscle fibers in TA muscle at 7 and 14 dpi detected by IHC staining and quantification of EMH$^+$ muscle fibers. *C*: IHC staining for Pax7$^+$ satellite cells in TA muscle at 7 and 14 dpi. The dotted-line inset on each image shows magnification of the area marked by the solid-line box. *D*: FACS for Lin$^-$/Sca-1$^-$/integrin α7$^+$ satellite cells in TA muscle 7 days after CTX injection. Data are mean ± SEM (n = 3). Scale bars = 200 μm. *P < 0.05, **P < 0.01 vs. control.

muscle regeneration in AMPKα1 mice might result from a combined effect of reduced satellite cell number and their myogenic differentiation.

AMPKα1 KO Promoted Fibrosis in Regenerating Muscle

Excessive fibrogenesis is associated with impaired muscle regeneration (31). To explore whether AMPKα1 KO affects fibrogenesis, we isolated Lin$^-$/Sca-1$^+$ fibro/adipogenic progenitor cells (10,32). Oil red O staining showed that adipogenesis was reduced in AMPKα1 KO compared with WT Lin$^-$/Sca-1$^+$ cells (Fig. 4*A*–*C*). In addition, newly formed adipocytes in AMPKα1 KO Lin$^-$/Sca-1$^+$ cells were clustered, suggesting a smaller percentage of cells undergoing adipogenic differentiation. Because fibro/adipogenic progenitor cells are dipotential with both adipogenic and fibrogenic capacity, the reduction in adipogenesis suggests a corresponding increase in fibrogenic commitment due to AMPKα1 KO. Indeed, the expression of TCF4, a marker of fibroblasts, was higher in AMPKα1 KO than in WT Lin$^-$/Sca-1$^+$ cells isolated from regenerating muscle (Fig. 4*D*), showing a larger population of fibroblasts in regenerating AMPKα1 KO muscle (33). These data are consistent with previous reports showing the inhibitory effect of AMPK on fibrogenesis in several examined tissues (34,35). In addition, a higher level of Tcf4 expression and more Tcf4$^+$ fibroblasts were detected in AMPKα1 KO than in WT TA muscle at 7 days postinjury (Fig. 4*E* and *F*). Trichrome staining at 14 days postinjury showed more collagen deposition in AMPKα1 KO TA muscle, clearly showing enhanced fibrogenesis in regenerating AMPKα1 KO muscle (Fig. 4*G*).

Despite the negative effect of excessive fibrosis on muscle regeneration, other studies showed that intramuscular

fibrogenic cells promote satellite cell proliferation (10,33,36). We then tested the expression level of IGF-I, a fibroblast-expressed growth factor stimulating satellite cell proliferation, in isolated nonmyogenic cells from muscle (37,38). IGF-I was expressed at a higher level in AMPKα1 KO than in WT nonmyogenic cells (Fig. 4*D*). Consistently, IGF-I expression was higher in AMPKα1 KO than in WT regenerating TA muscle (Fig. 4*E*). These results suggest that AMPKα1 KO enhances fibrosis, which might partially negate the reduced satellite cell number due to AMPKα1 KO in vivo.

Induced AMPKα1 KO in Adult Mice Before Muscle Injury Attenuated Muscle Regeneration

To eliminate the impact of AMPKα1 KO on muscle before injury and better understand the function of AMPKα1 during muscle regeneration, we used a conditional AMPKα1 KO, $R26^{Cre}/AMPK\alpha1^{fl/fl}$ mice with floxed AMPKα1 genes, which are deleted in response to tamoxifen treatment (Supplementary Fig. 1*A* and *B*). Three-month-old $R26^{Cre}/AMPK\alpha1^{fl/fl}$ mice were induced for AMPKα1 deletion followed by CTX-induced muscle injury in TA muscle. Muscle injury was induced immediately after induction of AMPKα1 KO to avoid differences in satellite cell density between tamoxifen-treated control ($AMPK\alpha1^{fl/fl}$) mice and conditional AMPKα1 KO ($R26^{Cre}/AMPK\alpha1^{-/-}$) mice at the time of injury. Nevertheless, fewer regenerated EMH^+ muscle fibers were observed in conditional AMPKα1 KO mice than in control mice at 7 days postinjury (Fig. 5*A* and *B*). Fourteen days after injury, the structure of TA muscle of control mice restored much better than that in conditional AMPKα1 KO mice (Fig. 5*A*). EMH staining showed that many thin EMH^+ muscle fibers remained in the muscle from conditional AMPKα1 KO muscle at 14 days postinjury, whereas only a few regular-shaped EMH^+ muscle fibers were seen in control mice (Fig. 5*B*). These data show that muscle regeneration in conditional AMPKα1 KO mice was less efficient than in control mice, independent of the initial satellite cell density.

Decreased satellite cell number was observed in muscle from conditional AMPKα1 KO mice compared with control mice at 7 and 14 days postinjury (Fig. 5*C*), which was confirmed by FACS data (Fig. 5*D*). In combination, these data show that lack of AMPKα1 affects muscle regeneration through reducing satellite cell proliferation and differentiation.

AMPKα1 KO Reduced Myogenic Capacity of Transplanted Satellite Cells In Vivo

To further examine the effect of AMPKα1 KO on myogenic capacity of satellite cells during muscle regeneration in vivo, we cotransplanted $AMPK\alpha1^{+/+}/EGFP$ satellite cells and $R26^{Cre}/AMPK\alpha1^{fl/fl}/DsRed$ satellite cells into regenerating TA muscle of WT mice. The mice were treated with tamoxifen each day starting on the same day of satellite transplantation until 2 days postinjury to induce AMPKα1 KO in transplanted $R26^{Cre}/AMPK\alpha1^{fl/fl}/DsRed$ satellite cells while avoiding the potential impact of AMPKα1 KO on establishing transplanted cells. Indeed, 2 days after satellite cell transplantation, no difference in the number of red and green fluorescent cells was observed (Fig. 6*A*), which indicated that the retention of transplanted $R26^{Cre}/AMPK\alpha1^{fl/fl}/DsRed$ and $AMPK\alpha1^{+/+}/EGFP$ satellite cells was not different. However, 14 days after satellite cell transplantation, a larger number of green muscle fibers than red muscle fibers was observed, showing the reduced myogenic capacity of transplanted satellite cells after AMPKα1 KO (Fig. 6*A* and *B*). In contrast, in the TA muscle of control mice, which were not treated with tamoxifen, the same number of green and red muscle fibers was observed at 14 days after transplantation, indicating an equal myogenic capacity of green and red satellite cells when AMPKα1 expression is intact (Supplementary Fig. 6). These data unequivocally demonstrate that AMPKα1 is important for the myogenesis of satellite cells during muscle regeneration.

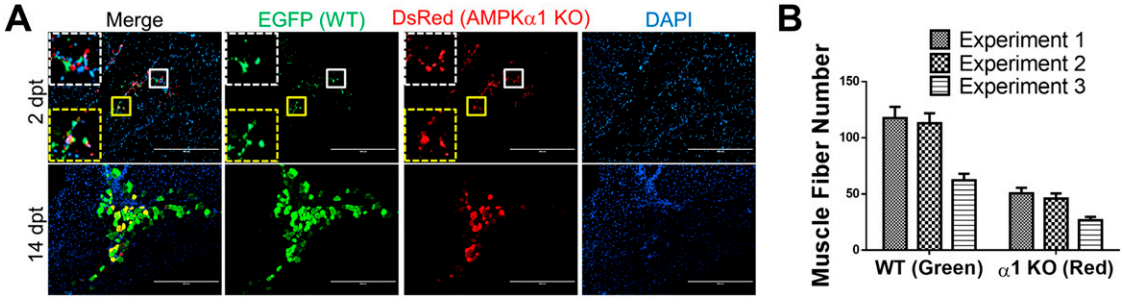

Figure 6—Reduced myogenesis in transplanted satellite cells with AMPKα1 KO during muscle regeneration. *A*: One day after CTX injection at TA muscle, 3×10^4 $AMPK\alpha1^{+/+}/EGFP$ satellite cells and 3×10^4 $R26^{Cre}/AMPK\alpha1^{fl/fl}/DsRed$ satellite cells were transplanted into each TA muscle of WT recipient mice. The recipient mice were treated with tamoxifen for 3 days from the day of transplantation. TA muscle was isolated at 2 days (top row) and 14 days (bottom row) after satellite cell transplantation and immunostained to identify muscle fibers derived from transplanted satellite cells. The dotted-line insets on each image show magnification of the corresponding areas marked by the solid-line boxes. Scale bars = 200 μm. *B*: Numbers of muscle fibers formed by transplanted myoblasts at 14 days after satellite cell transplantation in three independent experiments. Data are mean ± SEM (n = 3). dpt, days posttransplantation.

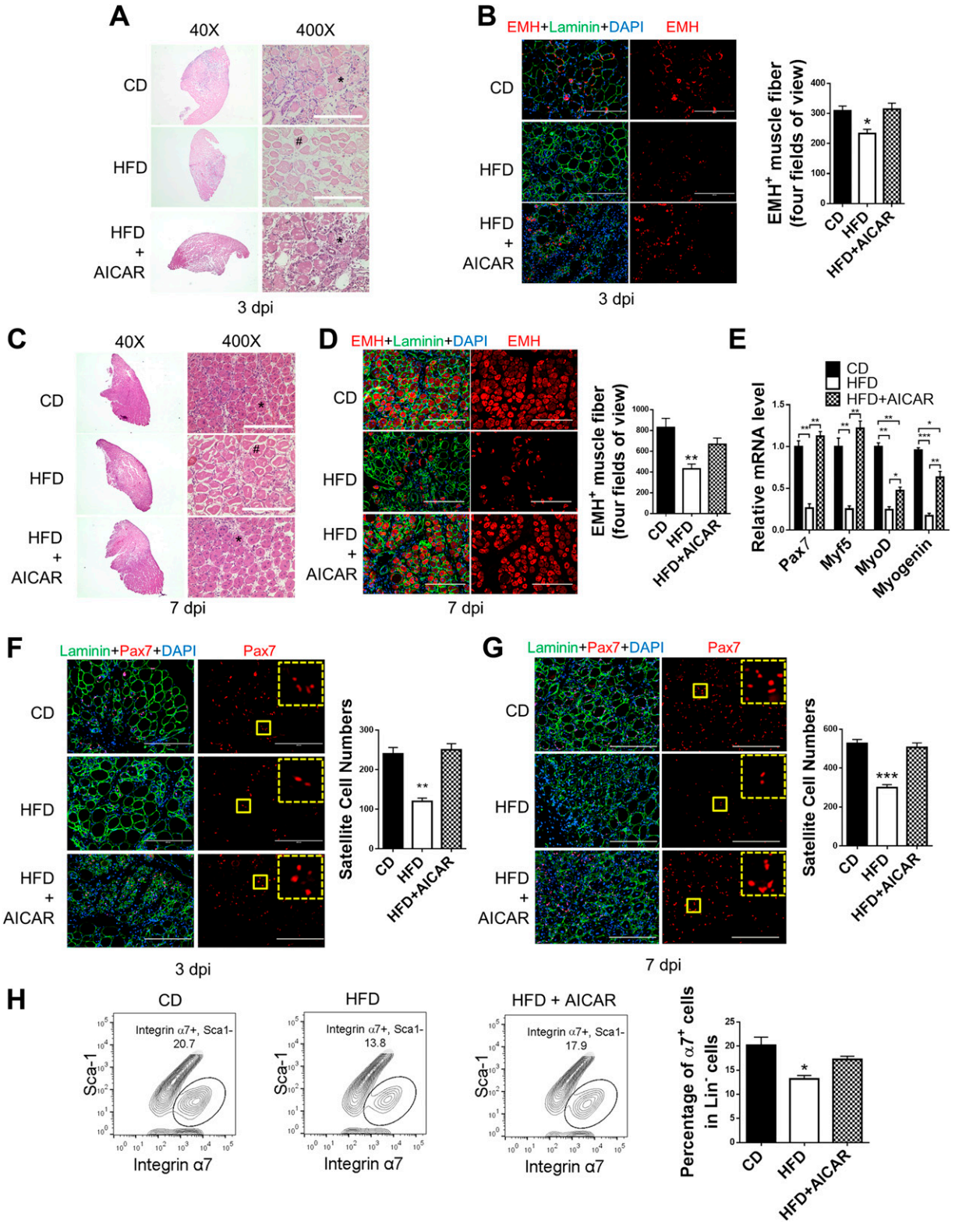

Figure 7—Attenuated AMPK activity and muscle regeneration in diet-induced obesity is rescued by AICAR treatment. TA muscle of mice fed a control diet (CD), obese mice fed a high-fat diet (HFD), and obese mice treated with AICAR (HFD + AICAR) were injured by CTX injection. Muscle was collected 1 h after the last AICAR treatment. *A*: Regeneration of TA muscle at 3 days postinjury (dpi) examined by H-E staining showing necrotic muscle fibers (#) and regenerating muscle fibers (*). *B*: IHC staining of EMH^+ muscle fibers in TA muscle at 3 dpi and quantification. *C*: Regeneration of TA muscle at 7 dpi examined by H-E staining showing necrotic muscle fibers (#) and regenerating muscle fibers (*). *D*: IHC staining of EMH^+ muscle fibers in TA muscle at 7 dpi and quantification. *E*: Pax7, Myf5, MyoD, and myogenin mRNA levels in TA muscle at 3 dpi. *F* and *G*: IHC staining of $Pax7^+$ satellite cells in TA muscle at 3 dpi (*F*) and 7 dpi (*G*) and quantification. The dotted-line inset on each image shows magnification of the area marked by the solid-line box. *H*: FACS for $Lin^-/Sca\text{-}1^-/integrin\ \alpha7^+$ satellite cells in TA muscle at 7 dpi. Data are mean ± SEM (n = 3). Scale bars = 200 μm. $^*P < 0.05$, $^{**}P < 0.01$, $^{***}P < 0.0001$ vs. control.

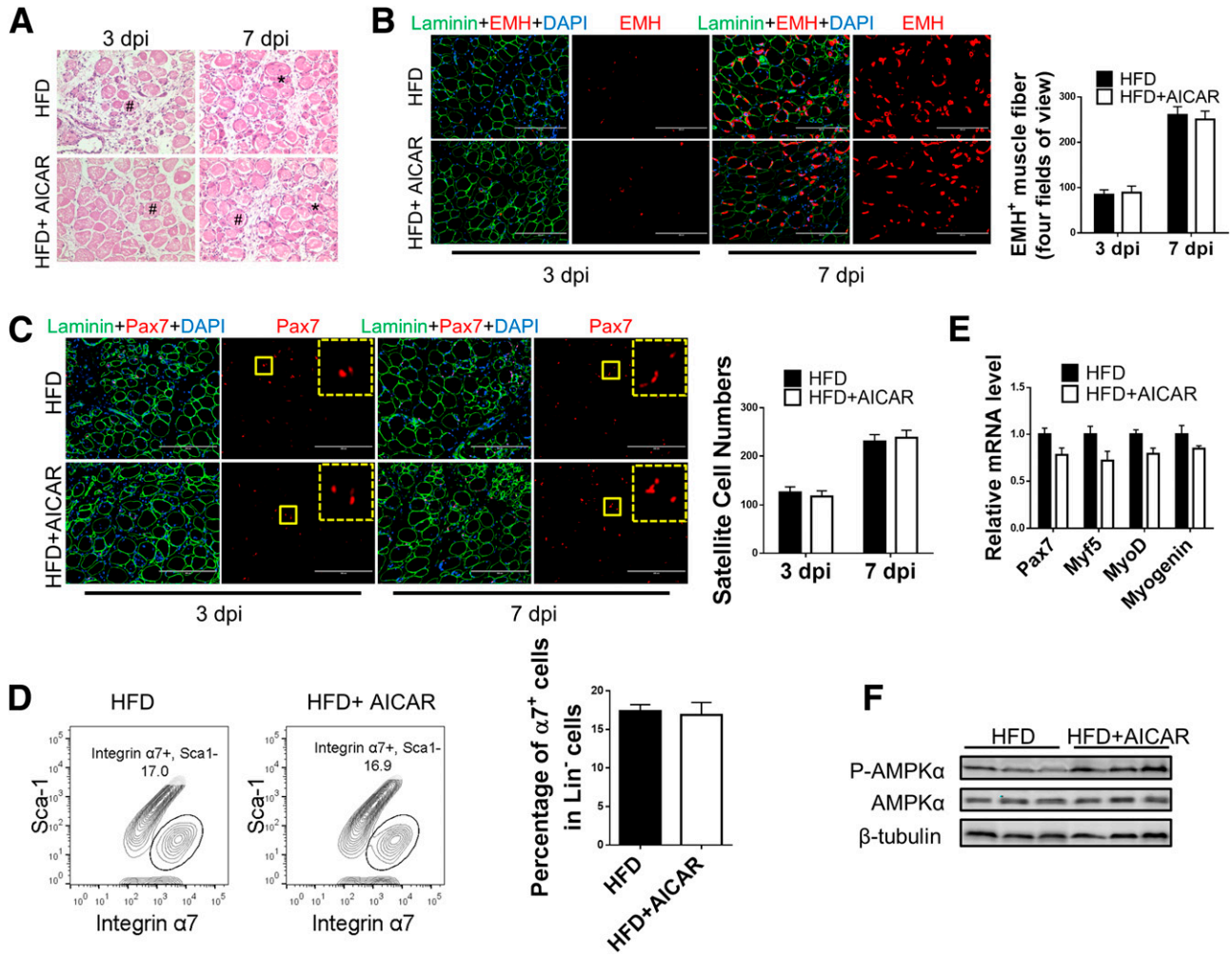

Figure 8—AMPKα1 deficiency in satellite cells abolishes the promotion effect of AICAR on muscle regeneration of obese mice. *Pax7^{Cre}/AMPKα1$^{fl/fl}$* were fed a high-fat diet (HFD). Satellite cell–specific AMPKα1 KO in *Pax7^{Cre}/AMPKα1$^{fl/fl}$* mice treated (HFD + AICAR) or not treated (HFD) with AICAR was achieved by tamoxifen injection. TA muscle was injured by CTX injection following tamoxifen injection. Muscle was collected 1 h after the last AICAR treatment. *A*: H-E staining of TA muscle at 3 and 7 days postinjury (dpi) showing necrotic muscle fibers (#) and regenerating muscle fibers (*). *B*: IHC staining of EMH$^+$ satellite cells in TA muscle at 3 and 7 dpi and quantification. *C*: IHC staining of Pax7$^+$ satellite cells in TA muscle at 3 and 7 dpi and quantification. The dotted-line inset on each image shows magnification of the area marked by the solid-line box. *D*: FACS for Lin$^-$/Sca-1$^-$/integrin α7$^+$ satellite cells at 7 dpi. *E*: Pax7, Myf5, MyoD, and myogenin mRNA levels in TA muscle at 3 dpi. *F*: Western blot analysis of p-AMPKα and AMPKα levels in muscle at 3 dpi. Data are mean ± SEM (n = 3). Scale bars = 200 μm.

AICAR Treatment Recovered Muscle Regeneration in Obese Mice Through AMPKα1 Activation

To further test whether elevated AMPK activity could promote muscle regeneration in obese mice, we treated obese mice with AICAR (250 mg/kg body weight/day i.p.), an AMPK activator, from 1 day before muscle injury until sampling days. AICAR treatment increased AMPK activity in whole regenerating muscle and satellite cells (Supplementary Fig. 7*A* and *B* and Fig. 1*D*). More EMH$^+$ muscle fibers were observed in mice treated with AICAR (Fig. 7*A–D*). Consistently, the transcription levels of Pax7, Myf5, MyoD, and myogenin were all enhanced in AICAR-treated mice at 3 days postinjury (Fig. 7*E*), and satellite cell numbers were also increased (Fig. 7*F–H*). We further used obese *Pax7^{Cre}/tdomato,EGFP* mice to trace satellite and derived cells; Pax7$^+$ satellite cell–derived muscle fibers were increased in AICAR-treated obese *Pax7^{Cre}/tdomato, EGFP* mice (Supplementary Fig. 4*A* and *B*). The rescued muscle regeneration in obese mice treated with AICAR further demonstrated that the reduced muscle regeneration in obese mice was caused by attenuated AMPK activity, which could be effectively recovered by enhancing AMPK activity. However, AICAR treatment failed to enhance myogenesis in control mice despite the increased p-AMPKα level in muscle in response to AICAR treatment, suggesting that elevated AMPK activity is only able to enhance muscle regeneration when AMPK activity is compromised (Supplementary Fig. 7*A*, *C–E*).

Because AICAR treatment improves whole-body metabolism in obese mice, to further test whether AICAR

improved muscle regeneration primarily through targeting satellite cells, obese $Pax7^{Cre}/AMPK\alpha1^{fl/fl}$ mice, where AMPKα1 is deleted specifically in satellite cells (Pax7-expressing cells) upon tamoxifen treatment, were used (Supplementary Fig. 1*C* and *D*). The promotion effect of AICAR treatment on muscle regeneration was not observed in mice lacking AMPKα1 in satellite cells, as indicated by unaltered EMH^+ muscle fiber numbers (Fig. 8*A* and *B*), satellite cell numbers (Fig. 8*C* and *D*), and Pax7, Myf5, MyoD, and myogenin expression (Fig. 8*E*) with and without AICAR treatment despite the elevated p-AMPKα level in injured muscle in response to AICAR treatment (Fig. 8*F*). These results show that AMPKα1 activity in satellite cells is required for the enhanced muscle regeneration in AICAR-treated obese mice.

DISCUSSION

Obesity has become an epidemic disease accompanied by many severe complications, including insulin resistance and cardiovascular disease (39,40). AMPK is an important regulator of metabolism that is activated when calories are restricted (15). Its activity is downregulated under the obese condition, and elevated AMPK activity alleviates obesity and its associated metabolic dysfunctions through promoting glucose uptake in muscle and increasing the sensitivity of animal to insulin (41–44). Muscle regeneration has been reported to be enhanced by calorie restriction, which may be due to enhanced AMPK activity, although direct evidence is lacking (45). We demonstrate that muscle regeneration in obese mice is impaired due to decreased AMPKα1 activity in satellite cells and that AMPKα1 KO reduces proliferation and myogenic capacity of satellite cells during muscle regeneration. On the contrary, fibrogenesis is enhanced in AMPKα1 KO mice. These data demonstrate for the first time in our knowledge the role of AMPKα1 in regulating both proliferation and differentiation of satellite cells during muscle regeneration.

We further tested the effectiveness of AMPK as a target to facilitate muscle regeneration in obese mice. AMPK activation induced by AICAR successfully improved muscle regeneration in the obese mice. Furthermore, KO of AMPKα1 in satellite cells abolished the promoting effect of AICAR treatment on muscle regeneration, strengthening the notion that the enhanced muscle regeneration in AICAR-treated obese mice is mainly due to elevated AMPKα1 activity in satellite cells. However, the unchanged muscle regeneration in mice fed the control diet in response to AICAR treatment suggests that AMPK activity at a level higher than its normal physiological level does not further enhance muscle regeneration. On the contrary, chronic AMPK activation in muscle may induce muscle atrophy, suggesting that more studies are required to optimize AMPK activity to promote muscle regeneration without inducing side effects (46).

In summary, we show that AMPKα1 is a key factor leading to impaired muscle regeneration in obese mice. AMPK is important in muscle regeneration because it increases the density of quiescent satellite cells, enhances satellite cell proliferation, and promotes satellite cell myogenic differentiation in regenerating muscle. Therefore, AMPK has multifaceted effects on muscle regeneration. The data have the following important clinical applications: *1*) AMPK activity is attenuated by a number of physiological factors, including obesity and diabetes, and *2*) drugs targeting AMPK are widely available as antidiabetic drugs, which may be used to activate AMPK to facilitate muscle regeneration in patients with obesity and diabetes.

Funding. This work was supported by National Institutes of Health grant 1R01-HD-067449 to M.D.

Duality of Interest. No potential conflicts of interest relevant to this article were reported.

Author Contributions. X.F. contributed to the experimental design and performance, data analysis, interpretation of the results, figure preparation, and drafting of the manuscript. M.Z., S.Z., M.F., and B.V. provided critical tools for the experiments. M.D. contributed to the experimental design, interpretation of the results, and drafting and final approval of the manuscript. M.D. is the guarantor of this work and, as such, had full access to all the data in the study and takes responsibility for the integrity of the data and the accuracy of the data analysis.

References

1. Schenk S, Horowitz JF. Acute exercise increases triglyceride synthesis in skeletal muscle and prevents fatty acid-induced insulin resistance. J Clin Invest 2007;117:1690–1698
2. Youn JY, Cai H. Fueling up skeletal muscle to reduce obesity: a TrkB story. Chem Biol 2015;22:311–312
3. Kennedy JW, Hirshman MF, Gervino EV, et al. Acute exercise induces GLUT4 translocation in skeletal muscle of normal human subjects and subjects with type 2 diabetes. Diabetes 1999;48:1192–1197
4. Armstrong RB, Warren GL, Warren JA. Mechanisms of exercise-induced muscle fibre injury. Sports Med 1991;12:184–207
5. Darr KC, Schultz E. Exercise-induced satellite cell activation in growing and mature skeletal muscle. J Appl Physiol (1985) 1987;63:1816–1821
6. Webster C, Blau HM. Accelerated age-related decline in replicative life-span of Duchenne muscular dystrophy myoblasts: implications for cell and gene therapy. Somat Cell Mol Genet 1990;16:557–565
7. Lepper C, Partridge TA, Fan CM. An absolute requirement for Pax7-positive satellite cells in acute injury-induced skeletal muscle regeneration. Development 2011;138:3639–3646
8. Kuang S, Kuroda K, Le Grand F, Rudnicki MA. Asymmetric self-renewal and commitment of satellite stem cells in muscle. Cell 2007;129:999–1010
9. Li H, Malhotra S, Kumar A. Nuclear factor-kappa B signaling in skeletal muscle atrophy. J Mol Med (Berl) 2008;86:1113–1126
10. Uezumi A, Fukada S, Yamamoto N, Takeda S, Tsuchida K. Mesenchymal progenitors distinct from satellite cells contribute to ectopic fat cell formation in skeletal muscle. Nat Cell Biol 2010;12:143–152
11. Bernasconi P, Torchiana E, Confalonieri P, et al. Expression of transforming growth factor-beta 1 in dystrophic patient muscles correlates with fibrosis. Pathogenetic role of a fibrogenic cytokine. J Clin Invest 1995;96:1137–1144
12. Renault V, Piron-Hamelin G, Forestier C, et al. Skeletal muscle regeneration and the mitotic clock. Exp Gerontol 2000;35:711–719
13. Allen RE, Boxhorn LK. Regulation of skeletal muscle satellite cell proliferation and differentiation by transforming growth factor-beta, insulin-like growth factor I, and fibroblast growth factor. J Cell Physiol 1989;138:311–315
14. Yablonka-Reuveni Z, Rudnicki MA, Rivera AJ, Primig M, Anderson JE, Natanson P. The transition from proliferation to differentiation is delayed in satellite cells from mice lacking MyoD. Dev Biol 1999;210:440–455

15. Zhang BB, Zhou G, Li C. AMPK: an emerging drug target for diabetes and the metabolic syndrome. Cell Metab 2009;9:407–416
16. Gulati AK, Swamy MS. Regeneration of skeletal muscle in streptozotocin-induced diabetic rats. Anat Rec 1991;229:298–304
17. Nguyen M-H, Cheng M, Koh TJ. Impaired muscle regeneration in ob/ob and db/db mice. ScientificWorldJournal 2011;11:1525–1535
18. Steinberg GR, Michell BJ, van Denderen BJ, et al. Tumor necrosis factor α-induced skeletal muscle insulin resistance involves suppression of AMP-kinase signaling. Cell Metab 2006;4:465–474
19. Stapleton D, Mitchelhill KI, Gao G, et al. Mammalian AMP-activated protein kinase subfamily. J Biol Chem 1996;271:611–614
20. Fu X, Zhao JX, Liang J, et al. AMP-activated protein kinase mediates myogenin expression and myogenesis via histone deacetylase 5. Am J Physiol Cell Physiol 2013;305:C887–C895
21. Fu X, Zhao JX, Zhu MJ, et al. AMP-activated protein kinase α1 but not α2 catalytic subunit potentiates myogenin expression and myogenesis. Mol Cell Biol 2013;33:4517–4525
22. Hayashi S, McMahon AP. Efficient recombination in diverse tissues by a tamoxifen-inducible form of Cre: a tool for temporally regulated gene activation/inactivation in the mouse. Dev Biol 2002;244:305–318
23. Zhao JX, Yue WF, Zhu MJ, Du M. AMP-activated protein kinase regulates beta-catenin transcription via histone deacetylase 5. J Biol Chem 2011;286:16426–16434
24. Lindholm CR, Ertel RL, Bauwens JD, Schmuck EG, Mulligan JD, Saupe KW. A high-fat diet decreases AMPK activity in multiple tissues in the absence of hyperglycemia or systemic inflammation in rats. J Physiol Biochem 2013;69:165–175
25. Gauthier M-S, O'Brien EL, Bigornia S, et al. Decreased AMP-activated protein kinase activity is associated with increased inflammation in visceral adipose tissue and with whole-body insulin resistance in morbidly obese humans. Biochem Biophys Res Commun 2011;404:382–387
26. Chazaud B, Brigitte M, Yacoub-Youssef H, et al. Dual and beneficial roles of macrophages during skeletal muscle regeneration. Exerc Sport Sci Rev 2009;37:18–22
27. Tidball JG, Villalta SA. Regulatory interactions between muscle and the immune system during muscle regeneration. Am J Physiol Regul Integr Comp Physiol 2010;298:R1173–R1187
28. Mounier R, Théret M, Arnold L, et al. AMPKα1 regulates macrophage skewing at the time of resolution of inflammation during skeletal muscle regeneration. Cell Metab 2013;18:251–264
29. Sambasivan R, Yao R, Kissenpfennig A, et al. Pax7-expressing satellite cells are indispensable for adult skeletal muscle regeneration. Development 2011;138:3647–3656
30. Blanco-Bose WE, Yao C-C, Kramer RH, Blau HM. Purification of mouse primary myoblasts based on α 7 integrin expression. Exp Cell Res 2001;265:212–220
31. Sato K, Li Y, Foster W, et al. Improvement of muscle healing through enhancement of muscle regeneration and prevention of fibrosis. Muscle Nerve 2003;28:365–372
32. Uezumi A, Ito T, Morikawa D, et al. Fibrosis and adipogenesis originate from a common mesenchymal progenitor in skeletal muscle. J Cell Sci 2011;124:3654–3664
33. Murphy MM, Lawson JA, Mathew SJ, Hutcheson DA, Kardon G. Satellite cells, connective tissue fibroblasts and their interactions are crucial for muscle regeneration. Development 2011;138:3625–3637
34. Handy JA, Saxena NK, Fu P, et al. Adiponectin activation of AMPK disrupts leptin-mediated hepatic fibrosis via suppressors of cytokine signaling (SOCS-3). J Cell Biochem 2010;110:1195–1207
35. Du J, Guan T, Zhang H, Xia Y, Liu F, Zhang Y. Inhibitory crosstalk between ERK and AMPK in the growth and proliferation of cardiac fibroblasts. Biochem Biophys Res Commun 2008;368:402–407
36. Joe AW, Yi L, Natarajan A, et al. Muscle injury activates resident fibro/adipogenic progenitors that facilitate myogenesis. Nat Cell Biol 2010;12:153–163
37. Sheehan SM, Allen RE. Skeletal muscle satellite cell proliferation in response to members of the fibroblast growth factor family and hepatocyte growth factor. J Cell Physiol 1999;181:499–506
38. Husmann I, Soulet L, Gautron J, Martelly I, Barritault D. Growth factors in skeletal muscle regeneration. Cytokine Growth Factor Rev 1996;7:249–258
39. Kahn SE, Hull RL, Utzschneider KM. Mechanisms linking obesity to insulin resistance and type 2 diabetes. Nature 2006;444:840–846
40. Van Gaal LF, Mertens IL, De Block CE. Mechanisms linking obesity with cardiovascular disease. Nature 2006;444:875–880
41. Watt MJ, Dzamko N, Thomas WG, et al. CNTF reverses obesity-induced insulin resistance by activating skeletal muscle AMPK. Nat Med 2006;12:541–548
42. Kola B, Grossman A, Korbonits M. The role of AMP-activated protein kinase in obesity. Front Horm Res 2008;36:198–211
43. Martin TL, Alquier T, Asakura K, Furukawa N, Preitner F, Kahn BB. Diet-induced obesity alters AMP kinase activity in hypothalamus and skeletal muscle. J Biol Chem 2006;281:18933–18941
44. Russell RR 3rd, Bergeron R, Shulman GI, Young LH. Translocation of myocardial GLUT-4 and increased glucose uptake through activation of AMPK by AICAR. Am J Physiol 1999;277:H643–H649
45. Cerletti M, Jang YC, Finley LW, Haigis MC, Wagers AJ. Short-term calorie restriction enhances skeletal muscle stem cell function. Cell Stem Cell 2012;10:515–519
46. Gordon SE, Lake JA, Westerkamp CM, Thomson DM. Does AMP-activated protein kinase negatively mediate aged fast-twitch skeletal muscle mass? Exerc Sport Sci Rev 2008;36:179–186